Available online at www.sciencedirect.com
SCIENCE DIRECT®
Journal of Non-Crystalline Solids 328 (2003) 183–191
JOURNAL OF NON-CRYSTALLINE SOLIDS
www.elsevier.com/locate/jnoncrysol

Refractive index measurements of planar chalcogenide thin film

Jacques M. Laniel [a,*], Jean-Michel Ménard [a], Karine Turcotte [a], Alain Villeneuve [a,1], Réal Vallée [a], Cédric Lopez [b], Kathleen A. Richardson [b,2]

[a] *Département de physique, génie physique et optique, Centre d'optique photonique et laser (COPL), Université Laval, Qué., Canada G1K 7P4*

[b] *School of Optics, Center for Research and Education in optics and Lasers (CREOL), University of Central Florida, 4000 Central Florida Boulevard, Orlando, FL 32816, USA*

Received 11 February 2003

Abstract

We report on the measurements of the refractive index of As–S–Se chalcogenide glasses near 1.55 μm. The measurements were made on annealed and non-annealed samples of thermally evaporated thin films. The data for two different series of glasses are presented: the compositions $As_{40}S_{60-x}Se_x$ and the compositions $As_xS_{(100-x)/2}Se_{(100-x)/2}$ where the ratio of sulfur to selenium is kept constant (1:1). It has been found that replacing sulfur by selenium in the first series increases the refractive index from 2.4 to 2.8 and increasing the arsenic content in the second series increases the refractive index. In all cases, it has been found that annealing the samples increase the refractive index. The accuracy in the refractive index measurement is ±0.2%.

PACS: 78.20.−e; 78.66.Jg; 78.20.Ci

1. Introduction

Over the past few years, many experimental studies have shown that chalcogenide glasses are promising materials for building high speed infrared communication integrated circuits [1]. These glasses possess interesting optical properties such as a good transmission in the 1–10 μm wavelength region. They also exhibit high photosensitivity which allows the writing of holographic patterns such as Bragg gratings [2]. These amorphous materials have a high linear [3] and non-linear refractive index [4]. Their non-linear refractive index is typically two orders of magnitude greater than that of silica. The possibility of doping these glasses with rare-earth conjugated to their low-phonon energy make them good candidates for optical amplification [5]. In order to

* Corresponding author. Tel.: +1-418 656 2131x6220; fax: +1-418 656 2623.
E-mail address: jmlaniel@phy.ulaval.ca (J.M. Laniel).
[1] Present adddress: ITF Optical Technologies Inc., 45 Montpellier Boulevard, Saint-Laurent, Qué., Canada.
[2] On leave at Schott Glass Technologies, Inc., 400 York Avenue, Duryea, PA 18643, USA.

0022-3093/$ - see front matter © 2003 Elsevier B.V. All rights reserved.
doi:10.1016/S0022-3093(03)00527-1

design an integrated circuit using one or more of these glasses, it is crucial to have a good knowledge of their linear optical properties. It is especially important since the value of the refractive index along with the dimensions of the structure will determine the spatial distribution of the propagating optical modes. Therefore, by choosing the right chalcogenide material, it is possible to engineer the mode profile in order to maximize the overlap with the active ions in the case of amplification or with the non-linear material in the case of non-linear optical switching.

Prior studies [3,4,6,7] have already reported linear refractive index measurements for certain chalcogenide glasses. In the present work, we have concentrated our study on thin films within the ternary arsenic (As), sulfur (S) and selenium (Se) system. Some basic measurements have already been done on these compositions, but none were precise enough for the efficient design of a waveguide since they were made using a Fresnel reflection technique, with a limit to precision of 1%. Furthermore, it is worth noting that integrated optical circuits require thin films [8,9]. It has been shown that the optical properties of bulk glasses are not always the same as those of thin films. This is mainly due to the deposition process which organizes the glass in a different manner in comparison to the bulk sample [8].

In this paper, we report results from a systematic study of eight chalcogenide glasses made of As–S–Se. The glass compositions examined in this work are shown in Fig. 1. Two series of glasses have been studied: the compositions #1 to #5 for which the ratio As/(S + Se) is kept constant (open circles) and the composition #3, #6 to #8 (closed circles) for which the ratio S/Se is kept constant (1:1) while the As content is decreasing. All of these compositions are known to form stable bulk glasses and in our previous investigations, no sign of crystallization was seen in evaporated films. The refractive indices of all these glasses have been measured for annealed and non-annealed thin films. The experimental method used for measuring the refractive index is based on a grating coupler setup [10]. This method has been preferred to the more common prism coupler experiment because it does not require putting in contact a prism with the film and therefore risking to damage it. Since the grating is etched on the surface of the substrate, the reproducibility of the results is increased. These measurements allow a comparison between the chalcogenide thin film and the chalcogenide bulk. This study also gives a quantitative evaluation of the refractive index changes after annealing of the chalcogenide films.

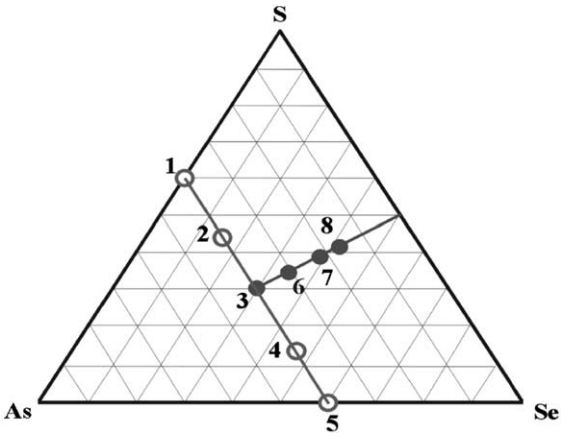

Fig. 1. Ternary diagram As–S–Se of studied glass composition. #1: $As_{40}S_{60}$, #2: $As_{40}S_{15}Se_{45}$, #3: $As_{40}S_{30}Se_{30}$, #4: $As_{40}S_{45}Se_{15}$, #5: $As_{40}Se_{60}$, #6: $As_{32}S_{34}Se_{34}$, #7: $As_{24}S_{38}Se_{38}$, #8: $As_{18}S_{41}Se_{41}$.

2. Experimental procedures

2.1. Grating coupling experiment

We used a grating coupling experiment in order to measure the refractive index of each glass [10]. Since any transparent thin film of sufficiently high index can be used as a planar waveguide capable of supporting optical propagating modes, it is possible to excite these modes with the help of a grating. This is made possible by phase-matching an incident beam with the supported modes of the structure via the diffracted order of the grating. Therefore, each mode will be associated with a coupling angle. The relationship between the coupling angle and the propagating constant of the waveguide is given by relation (1):

$$k_0 \sin\theta_{p,m} + m\frac{2\pi}{\Lambda} = \beta_p, \tag{1}$$

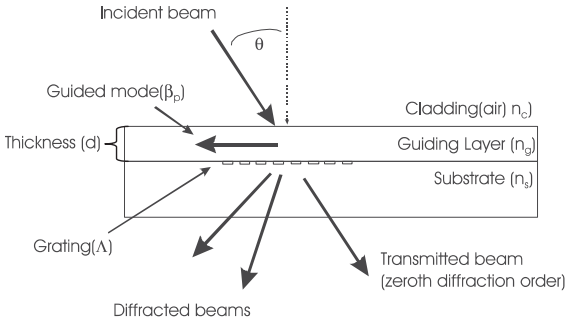

Fig. 2. Grating coupler configuration. The guiding layer is deposited onto a glass substrate. The grating has been etched on the substrate. The incident beam couples within the waveguide by phase matching with one of the diffraction order of the grating.

where $k_0 = 2\pi/\lambda$ is the wave vector of the incident beam, Λ is the grating period and β_p is the propagating constant of mode p. So, for each mode p of the structure and diffraction order m, there is an associated coupling angle $\theta_{p,m}$. The propagation constant β_p is obtained from the dispersion relation of the waveguide. The waveguide structure we used is shown in Fig. 2.

The dispersion relation of the planar waveguide [11] is function of the refractive index of each media (the cladding n_c, the guiding layer n_g and the substrate n_s) and the thickness d of the guiding layer. The relationship is also dependent on the polarization state of the exciting light. For the TE mode, the dispersion relation is given by relation (2).

$$v\sqrt{1-b_p} = p\pi + \tan^{-1}\sqrt{\frac{b_p}{1-b_p}} + \tan^{-1}\sqrt{\frac{b_p+a}{1-b_p}}. \tag{2}$$

The normalized frequency v, the normalized effective index b_p of mode labeled p and the asymmetry factor a are defined by relations (3)–(5).

$$v = k_0 d\sqrt{n_g^2 - n_s^2}, \tag{3}$$

$$b_p = \frac{n_{\mathrm{eff},p}^2 - n_s^2}{n_g^2 - n_s^2}, \tag{4}$$

$$a = \frac{n_s^2 - n_c^2}{n_g^2 - n_s^2}. \tag{5}$$

The effective index of mode p is related to the propagation constant by $\beta_p = k_0 n_{\mathrm{eff},p}$. The experimental measurements of each coupling angle give the propagation constants for the modes β_p of the planar waveguide. Then, by numerical inversion of the dispersion relation given by relation (2), one can obtain the refractive index and the thickness of the planar waveguide. This is made possible only if the refractive index of the substrate and the grating period is known with good accuracy. The experimental setup used to measure the coupling angle is shown in Fig. 3.

The detection of the coupling angles is based on the measurement of the transmission in the zeroth order of diffraction. When the incident angle coincides with a coupling angle, the incident beam will couple to a propagating mode of the planar waveguide. Therefore, there will be a significant decrease in the transmission of the zeroth order. The coupling angle will then be associated with a localized decrease in the transmission of the zeroth order while rotating the sample. The intensity and state of polarization of the incident beam are controlled by a wave plate and a polarizer. The powers were measured with two InGaAs detectors. The rotation of the sample and the detection were controlled by a computer.

2.2. Sample preparation

The bulk materials were prepared by conventional melt quenching in an evacuated silica ampoule. High purity raw materials (As (99.9995%), S (99.999%) and Se (99.99%)) were used to prepare between 7 and 12 g of chalcogenide glasses. After being weighed in a nitrogen atmosphere within a dry box, the batch was placed inside a silica tube pretreated for 8 h at 900 °C in a furnace to remove surface moisture. The tube was evacuated and a cold trap was placed on the process line to capture gases. A first treatment of 4 h at 105 °C was applied to the tube containing the raw materials. For each glass, there has been a distillation of the raw materials performed in a four zone furnace.

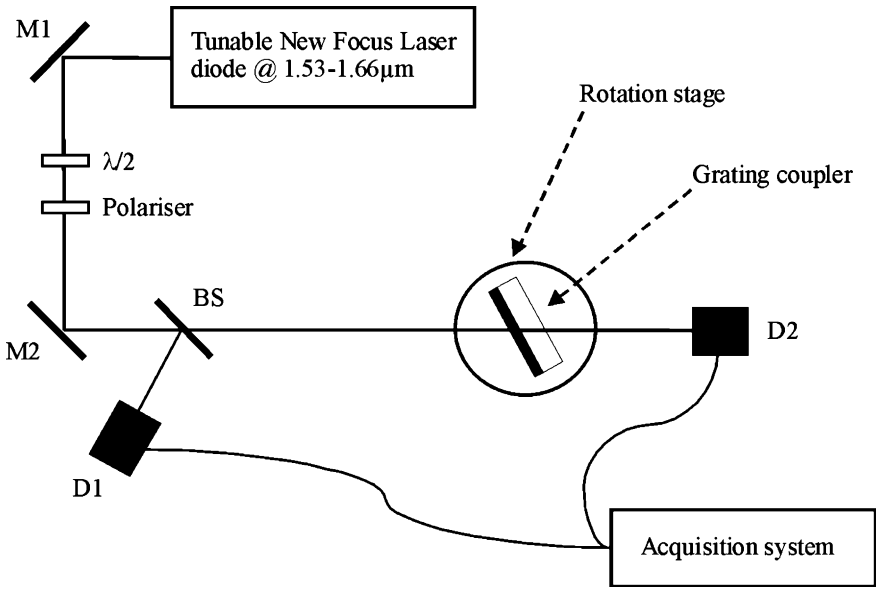

Fig. 3. Experimental setup used for measuring the coupling angles. The grating coupler is mounted on a precision rotation stage. The input and output intensities are detected by InGaAs detectors (D1 and D2). The state of polarization and intensity of the incident beam are controlled by a half-wave plate ($\lambda/2$) and a polarizer. The experiment is controlled by computer. The laser source is a New Focus Inc. Velocity tunable laser diode operating between 1.53 and 1.66 μm. The accuracy of the rotation stage is 200 steps/degree.

A methane–oxygen torch was used to seal the tube, which was then placed in a rocking furnace to be heated and homogenized overnight (18 h) at a melting temperature between 800 and 850 °C depending on the composition of the sample. The tube was air quenched from a determined quenching temperature after being removed from the furnace. The sealed ampoule was annealed at a temperature of 50 °C below the glass transition temperature (T_g) in the furnace under an argon flow. The samples were then cut in smaller pieces. The composition of the bulk glasses were confirmed by a Cameca SX100 electron probe microanalyzer. The results obtained confirmed that the compositions lie within 2% of specified parameters.

The thin films were prepared by thermal evaporation of small broken pieces of the bulk glass. The deposition was made at a rate of ~20–30 Å/s under a pressure of 10^{-7} Torr onto a silica substrate. The substrate was rotated for better homogeneity and unheated. The typical thicknesses deposited are around ~2.5 μm. The actual thickness values were measured using a mechanical profilometer in order to orient the numerical fit. The samples were annealed in vacuum at 120 °C for 2 h. In order to allow for grating coupling, we used a silica substrate on which a grating had been previously etched. The grating used was in fact a phase mask used normally for Bragg grating inscription. The period of the grating used was 0.679 μm. Such a configuration allows coupling in four to five optical modes and has shown to give reliable results.

3. Results

The coupling angles have been measured at wavelengths around 1.55 μm. The laser used was a New Focus Velocity tunable diode laser operating between 1.528 and 1.658 μm. The measurements were performed at four wavelengths i.e. 1.530, 1.550, 1.575 and 1.600 μm. Since the accuracy of the method does not allow a measurement of the natural birefringence of the deposited films, we only used the TE polarization configuration for exciting the modes of the planar waveguide. We

Table 1
Refractive index for each composition in the case of annealed and non-annealed thin films given at 1.550 μm

Glass number	1	2	3	4	5	6	7	8
Annealed	2.405	2.464	2.571	2.677	2.832	2.541	2.465	2.375
Non-annealed	2.344	2.410	2.495	2.627	2.771	2.504	2.445	2.367

The uncertainty on the experimental values is ±0.2%.

summarize in Table 1, the refractive indices obtained for all eight compositions in the case of annealed and non-annealed samples at 1.550 μm. The refractive indices obtained at 1.530, 1.575 and 1.600 μm were within the experimental uncertainty and the natural dispersion of the materials. The uncertainty on the experimental values is ±0.2%.

Let us now consider the evolution of the refractive index as a function of different concentrations. Figs. 4 and 5 show the refractive index for the two series of glasses as depicted in Fig. 1. More specifically, Fig. 4 shows the refractive index when the composition varies from $x = 0$ to 60 mol% in $As_{40}S_{60-x}Se_x$. This is the case where the As content is kept constant while the S atoms are systematically replaced by Se atoms. Fig. 5 shows the case for which the composition goes from $x = 18\%$ to 40% in $As_xS_{(100-x/2)}Se_{(100-x/2)}$ where the S/Se ratio is kept constant to one and the arsenic composition is varied from 18% to 40%.

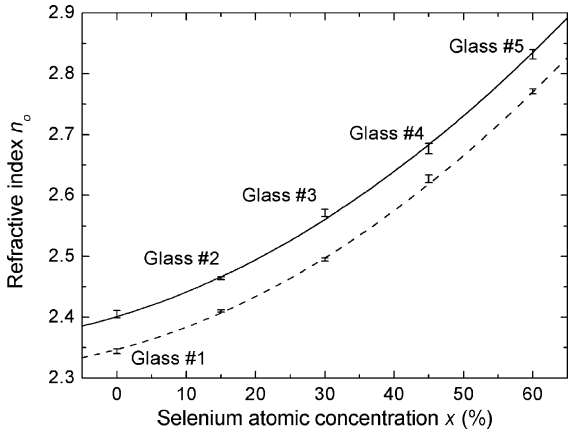

Fig. 4. Refractive index of glass #1 to #5 ($As_{40}S_{60-x}Se_x$) of the ternary diagram at 1.55 μm as a function of selenium atomic concentration. Straight line represents numerical fit for annealed samples and dotted line represents numerical fit for non-annealed samples.

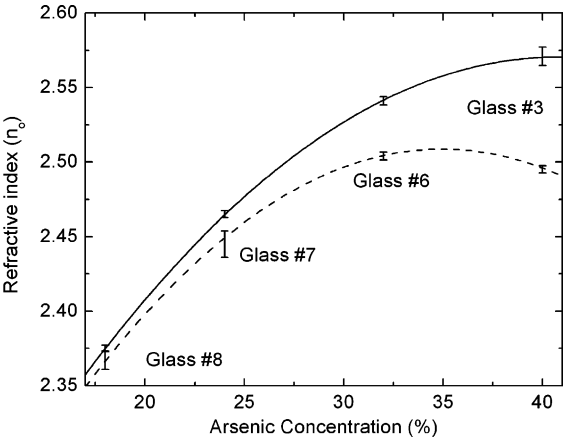

Fig. 5. Refractive index of glass #3, #6 to #8 ($As_xS_{100-x/2}Se_{100-x/2}$) of the ternary diagram at 1.55 μm as a function of arsenic atomic concentration. Straight line represents numerical fit for annealed samples and dotted line represents numerical fit for non-annealed samples.

The results presented in Figs. 4 and 5 have been fitted to a second order polynomial of the form $y = A + Bx + Cx^2$ in order to get empirical relations. The variable x represents the selenium atomic concentration in percent for glasses #1 to #5 and it represents the arsenic atomic concentration in percent for glasses #3, #6 to #8. These relations are useful for waveguide design since one can calculate the concentration needed for a specific refractive index. The results for the fit are presented in Table 2.

4. Discussion

In the following discussion, we refer to a previous work [3] in order to analyze and better understand the results we have obtained in chalcogenide thin films. The optical properties of

Table 2
Results for the numerical fit of the experimental values shown in Figs. 4 and 5

Material	Meaning of x	A	B	C	R
Glass #1 to #5 non-annealed	[Se], [As] = 40%	2.347	3.0×10^{-3}	6.7×10^{-5}	0.99934
Glass #1 to #5 annealed	[Se], [As] = 40%	2.401	3.4×10^{-3}	6.4×10^{-5}	0.99833
Glass #3, #6 to #8 non-annealed	[As], [S]/[Se] = 1	1.904	34.6×10^{-3}	-49.5×10^{-5}	0.99949
Glass #3, #6 to #8 annealed	[As], [S]/[Se] = 1	1.943	30.8×10^{-3}	-3.78×10^{-4}	0.99997

The fit was performed according to the empirical formula $y = A + Bx + Cx^2$. R is the regression coefficient for each numerical fit.

the eight glasses under investigation here have been characterized in bulk form by Cardinal et al., who reported linear and non-linear refractive index measurements of the glasses. They also reported absorption and Raman spectra and the density for each compound. Note that their results were obtained for bulk materials as opposed to ours on thin films.

The refractive index of a material is determined by the different electronic bonds from which it is composed. The As–S–Se chalcogenide glasses have a basic pyramidal unit made of AsX_3 with a triangular base composed of either sulfur or selenium (X = S or Se). In the case of stoichiometric compounds (glasses #1 to #5: $As_{40}S_{100-x}Se_x$), the pyramidal structure is in principle reproduced in the whole glass matrix and each chalcogen is linked to another arsenic, which is the top of another pyramidal unit, with no homopolar (like atom) bonds. In the case where the glass is not stoichiometric (glasses #6 to #8), i.e. as the molar arsenic concentration is reduced from 40% down to 18%, Raman spectroscopy [3] has shown that there is appearance of homopolar S–S, Se–Se and heteropolar S–Se bonds inside the glasses.

It is known that the value of the band gap in chalcogenide glasses is determined by the energy difference between the non-bonding valence band and the anti-bonding conduction band and not by the bond between the chalcogen and the arsenic atoms [12]. This is a typical property of chalcogenide amorphous solid.

Keeping the structure of the chalcogenide glasses in mind, we take a closer look at the experimental results for the stoichiometric glasses. Referring to Fig. 4, Cardinal et al. reported a similar evolution of refractive index in the bulk material when the As content is kept constant and the S atoms are replaced by Se ones. Their measurements showed that replacing sulfur atoms by selenium atoms decreases the value of the band gap from 2.1 eV for As_2S_3 down to 1.5 eV for As_2Se_3. According to the dispersion properties given by the classical electron-oscillator model [13], $n_0^2 - 1$ is scaling as $1/E_g^2$ where n_0 is the refractive index at a fixed wavelength and E_g is the band gap energy. The increase shown in the refractive index in Fig. 4 can be qualitatively explained by the shift of the band gap. This increase of the refractive index can also be explained by an increase of the total polarizability of the material when the sulfur atoms are replaced by selenium. A recent work by González-Leal et al., showed a relationship between the refractive index of a chalcogenide glass and its chemical content [7]. The Lorentz–Lorenz relationship [14] was used in order to study the evolution of the refractive index as a function of the selenium volumetric molar concentration for a fixed wavelength. Fig. 6 shows the dependence of $(n_0^2 - 1)/(n_0^2 + 2)$ calculated from Table 1 as a function of the selenium volumetric molar concentration for the case of annealed and non-annealed thin films. We have included in Fig. 6 the results for bulk samples at 1.6 μm taken by Cardinal et al. [3].

One sees that the relationship is not linear as the Lorentz–Lorenz relationship predicts for annealed and non-annealed thin films. We see that the bulk refractive indices follow more closely a linear relationship. This behavior can be explained by the fact that the Lorentz–Lorenz relationship may oversimplify the interaction inside the thin films. A

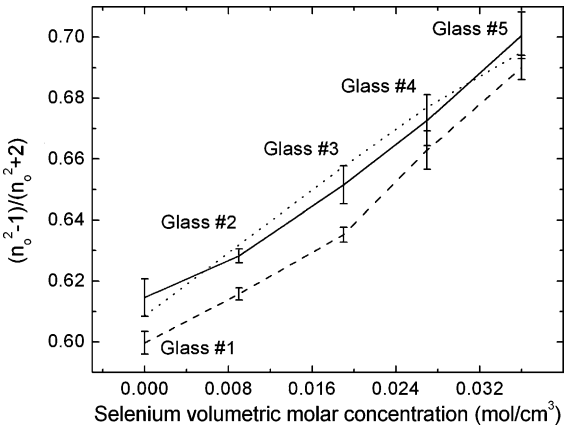

Fig. 6. Relation between the refractive index and the selenium volumetric molar concentration for glasses having a constant arsenic atomic concentration (40%). The sulfur atoms are being replaced by selenium ones (glasses #1 to #5 as shown in Fig. 1). Straight line represents annealed samples, dashed line non-annealed samples at 1.55 μm and dotted line represents bulk sample at 1.6 μm [3].

more complete model would include a better understanding and modeling of the different components contributing to the total polarization inside the material. Such modeling would require studying the quantum properties of the outer electronic shell of bonding sulfur and selenium with arsenic in order to calculate the energy levels of the anti-bonding and non-bonding bands. Such an analysis was outside the scope of this experimental report.

In the case where the concentration of sulfur and selenium was kept constant while varying the arsenic concentration from 18% up to 40% (from glass #8 to #6 and then #3 in the ternary diagram in Fig. 1), we saw an increase of the refractive index for both annealed and non-annealed thin films, as previously reported by Cardinal et al. for the bulk chalcogenide. Their absorption measurements have shown that for glasses #3, #6 to #8, there is no change in the value of the bang gap. This behavior can be explained by the fact that since the band gap is determined by the sulfur and selenium concentration, keeping constant the chalcogen concentration ratio (S/Se) to first order, keeps the band gap unchanged even though the arsenic concentration is varying. Taking this fact in account, it is not possible here to explain the change in the refractive index from one composition to another by a scaling of the band gap. According to the Lorentz–Lorenz relation, the factor $(n_0^2-1)/(n_0^2+2)$ is proportional to the molar volumetric concentration of arsenic of each glass since the ratio of sulfur and selenium atoms is kept constant. Fig. 7 shows the evolution of the Lorentz–Lorenz relation as a function of the volumetric molar concentration of arsenic for glasses #3, #6 to #8.

Although the refractive index is proportional to the volumetric molar concentration of arsenic, the relation is far from being linear. This might be explained qualitatively by the appearance of S–S and Se–Se and possibly S–Se bonds inside the glass matrix. The presence of such bonds will create new components to the polarization that our simple model does not take in account. These modifications will influence the refractive index and will perturb the evolution of the refractive index from one composition to another.

All chalcogenide thin films have exhibited a clear increase of the value of their refractive index after annealing. The refractive index increase was of the order of 2% for glasses #1 to #5 and less

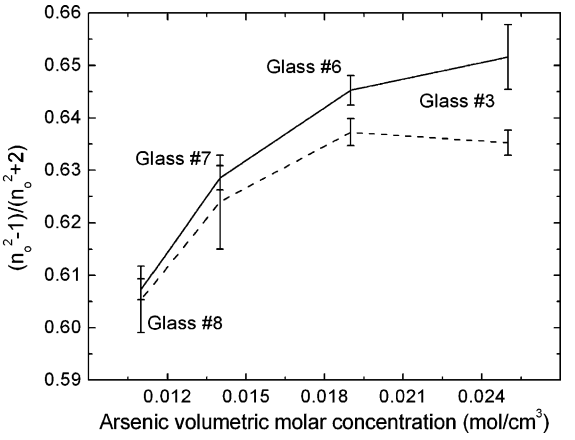

Fig. 7. Relation between the refractive index at a fixed wavelength (1.55 μm) and the arsenic volumetric molar concentration for glasses having equal concentration of sulfur and selenium (S/Se = 1) while varying the arsenic concentration (glass #3, #6 to #8). Straight line represents annealed samples and dotted line non-annealed samples.

than 2% for glasses #3, #6 to #8. A closer look at Figs. 4 and 5 shows that the refraction index increase is not the same for all glass compositions. For the stoichiometric glasses (#1 to #5), we see that the increase is constant for all concentrations. However, in the case of glasses for which the arsenic concentration was changed, the refractive index change depends strongly on the composition of the glass. This is consistent with the annealing effects and their dependence on network structure; greater chalcogen-containing films have more free volume flexibility to arrange during deposition and re-arrange, upon annealing. Similarly, larger As-containing materials possess more three-coordinated species, are more rigid and have less chance for reorganization. The as-deposited configuration (determined by deposition conditions and the extent from equilibrium the glass is prior to annealing), will also contribute to the extent of free volume/property change upon annealing.

Such an increase of the refractive index has already been observed in $As_{40}S_{60}$ by Yang et al. [15] where a clear red-shift of the band gap was reported leading to an increase of the refractive index in the infrared region. One can understand the processes causing the changes in the optical properties by looking at the structural changes inside the material before and after annealing. A previous comparative study between bulk and thermally evaporated thin films showed that non-annealed films contained As_4S_4 molecules [8]. The results also showed that annealing thin film at a temperature below its T_g allows the glass to relax and incorporate the As_4S_4 into the glass matrix. This was also confirmed by Raman spectroscopy measurements, which have shown that annealing the film actually reduces the As_4S_4 subunits [9]. The dissolution of the As_4S_4 inside the glass matrix changes the optical properties of the glasses. The changes in the absorption spectrum caused by an annealing of the thin film has already been characterized in our research group [16] and showed a red-shift of the band gap for the $As_{40}S_{60}$. According to the Kramers–Krönig relations, this red-shift will cause an increase in the refractive index in the infrared region and explains the behavior of the chalcogenide films when annealed.

5. Conclusion

In conclusion, we have precisely measured (with an uncertainty of ±0.2%) the refractive index of eight As–S–Se chalcogenide glasses based thin films in the 1.550 μm telecommunication wavelength region. The refractive indices for each glass have been obtained by means of a grating coupling experiment. We have shown that for the stoichiometric compositions, which consist of replacing sulfur atoms by selenium atoms while keeping the arsenic concentration constant (40 mol%), the refractive index increases from ~2.4 to ~2.8. We have also shown that for the case of equal concentration of sulfur and selenium atom (S/Se = 1), increasing the arsenic concentration from 14% up to 40 mol% increases the refractive index from ~2.38 up to ~2.6. For each glass, we measured an increase of the refractive index after annealing the thin film of the order of ~2% for the stoichiometric glasses (#1 to #5) and less than 2% for glasses #3, #6 to #8.

Acknowledgements

The authors would like to thank R. Piché for technical support, EXFO Electro-Optical Engineering Inc. and Lucent Technologies Inc. for their support. This work was supported by a strategic grant from the Natural Sciences and Engineering Research Council of Canada (NSERC). J.M.L. acknowledges a scholarship from NSERC.

References

[1] J.S. Sanghera, I.D. Aggarwal, J. Non-Cryst. Solids 256&257 (1999) 6.
[2] A. Saliminia, T. Galstian, A. Villeneuve, É.J. Knystautas, M.A. Duguay, K.A. Richardson, J. Opt. Soc. Am. B 17 (2000) 1343.
[3] T. Cardinal, K.A. Richardson, H. Shim, A. Schulte, R. Beatty, K. Le Foulgoc, C. Meneghini, J.F. Viens, A. Villeneuve, J. Non-Cryst. Solids 256&257 (1999) 353.
[4] J.M. Harbold, F.Ö. Ilday, F.W. Wise, J.S. Sanghera, V.Q. Nguyen, L.B. Shaw, I.D. Aggarwal, Opt. Lett. 27 (2002) 119.
[5] C. Meneghini, J.F. Viens, A. Villeneuve, É.J. Knystautas, M.A. Duguay, K.A. Richardson, J. Opt. Soc. Am. B 15 (1998) 1305.

[6] K. Petkov, P.J.S. Ewen, J. Non-Cryst. Solids 249 (1999) 150.
[7] J.M. González-Leal, R. Prieto-Alcón, J.A. Angel, E. Márquez, J. Non-Cryst. Solids 315 (2003) 134.
[8] A.J. Apling, A.J. Leadbetter, A.C. Wright, J. Non-Cryst. Solids 23 (1977) 364.
[9] A. Schulte, C. Rivero, K. Richardson, K. Turcotte, V. Hamel, A. Villeneuve, T. Galstian, R. Vallée, Opt. Commun. 198 (2001) 125.
[10] M. Nevière, E. Popov, R. Reinisch, G. Vitrant, Electromagnetic Resonances in Nonlinear Optics, Gordon and Breach, 2000, 389p.
[11] D.L. Lee, Electromagnetic Principles of Intergrated Optics, John Wiley, 1986, 331p.
[12] R. Zallen, The Physics of Amorphous Solids, John Wiley & Sons, Toronto, 1983, 304p.
[13] A.E. Siegman, Lasers, University Science Books, 1986, 1283p.
[14] R.W. Boyd, Nonlinear Optics, Academic Press, 1992, 439p.
[15] C.Y. Yang, M.A. Paesler, D.E. Sayers, Phys. Rev. B 36 (1987) 9160.
[16] Meneghini, Chiara, Dispositifs photoniques plans à base de verres chalcogénures, PhD thesis, Université Laval, 2000, 150p.